

Facile One-Pot Coupling–Aminovinylation Approach to Push–Pull Chromophores: Alkyne Activation by Sonogashira Coupling[†]

Alexei S. Karpov, Frank Rominger,[‡] and Thomas J. J. Müller*

Organisch-Chemisches Institut der Ruprecht-Karls-Universität Heidelberg, Im Neuenheimer Feld 270, D-69120 Heidelberg, Germany

thomas_j.j.mueller@urz.uni-heidelberg.de

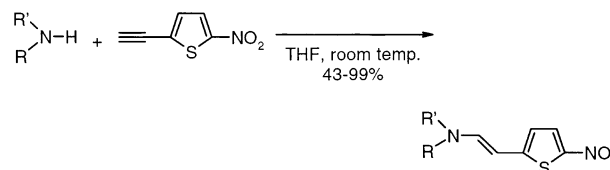
Received September 24, 2002

A straightforward coupling–aminovinylation sequence of terminal alkynes **1**, electron-deficient heteroaryl halides **2**, and secondary amines **4** furnishes highly solvochromic push–pull chromophores **5** in good yields. Semiempirical calculations (PM3) suggest that the aminovinylation proceeds in a stepwise fashion through a zwitterionic intermediate with a final rate-determining intramolecular protonation. Crucial parameters for the success of the amine addition are the relative LUMO energies and the charge distribution at the β -alkynyl carbon atom.

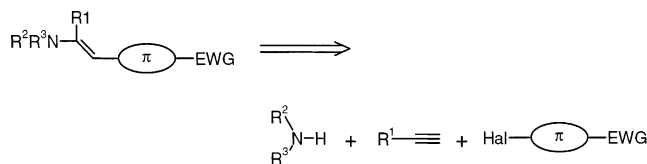
Introduction

The search for novel structural motifs with pronounced nonlinear optical properties and their practical synthesis are still ongoing challenges because the demand for tailor-made chromophores for numerous photonic applications is rapidly increasing.¹ Structurally and theoretically,^{1d} the push–pull substitution of organic chromophores has been recognized as a prerequisite and is a well-established basis for designing novel chromophores. However, the development of short chromophores with high dipole moments and, as a consequence, with high β -values overcoming the disadvantages of long and extended π -systems (i.e., bathochromic absorption, efficiency–transparency tradeoff) remains a challenge. In comparison to related benzoid systems, thienyl-based chromophores display remarkably higher hyperpolarizabilities^{1a,2} but also significantly red-shifted absorption bands. Thus, thienyl-based push–pull chromophores have been shown to exhibit excellent NLO properties.³ Recently, we illustrated that the high polarizability of thiophenes can synergistically be exploited for both synthesis and electronic properties of NLO target mol-

SCHEME 1. Aminovinylation of 5-Ethynyl 2-nitrothiophene



SCHEME 2. Retrosynthetic Analysis of Push–Pull Chromophores Based upon an in Situ Alkyne Activation



ecules.⁴ The effect of the strongly electron-withdrawing nitro group is efficiently transmitted through the thiophene core and concomitantly activates alkynes toward Michael-type additions of secondary amines to furnish β -aminovinyl nitrothiophenes, a novel class of push–pull chromophores with remarkable NLO responses and favorable glass-forming properties (Scheme 1).⁴

As part of our program to study and devise novel modes of alkyne activation⁵ initiated by catalytic C–C bond-forming reactions with the prospect of new MCR (multi-component reaction) methodologies, we report an extension of this facile β -aminovinyl nitrothiophene synthesis to a one-pot Sonogashira coupling–aminovinylation sequence.

Results and Discussion

The Sonogashira alkynylation is a fairly mild synthesis of internal alkynes, simultaneously tolerating a wide

(4) Müller, T. J. J.; Robert, J. P.; Schmälzlin, E.; Bräuchle, C.; Meerholz, K. *Org. Lett.* **2000**, *2*, 2419–2422.

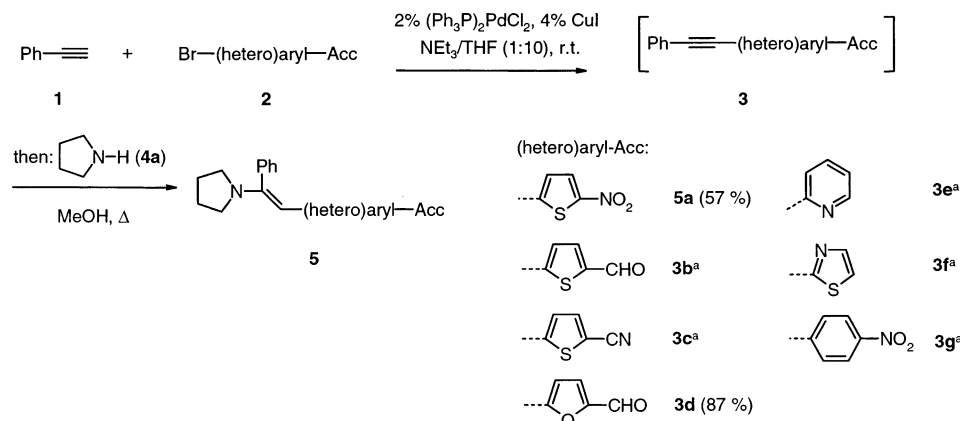
[†] Dedicated to Prof. Dr. K. H. Dötz on the occasion of his 60th birthday.

[‡] X-ray structure analysis.

(1) For recent reviews on NLO materials see, e.g.: (a) Long, N. J. *Angew. Chem., Int. Ed. Engl.* **1995**, *34*, 6–20. (b) Marder, S. R.; Perry, J. W. *Adv. Mater.* **1993**, *5*, 804–815. (c) Nie, W. *Adv. Mater.* **1993**, *5*, 520–545. (d) Kanis, D. R.; Ratner, M. A.; Marks, T. J. *Chem. Rev.* **1994**, *94*, 195–242. (e) Marks, T. J.; Ratner, M. A. *Angew. Chem., Int. Ed. Engl.* **1995**, *34*, 155–173. (f) Wolff, J. J.; Wortmann, R. *Adv. Phys. Org. Chem.* **1999**, *32*, 121–217.

(2) (a) Jen, A. K. Y.; Rao, V. P.; Wong, K. Y.; Drost, K. J. *J. Chem. Soc., Chem. Comm.* **1993**, 90–92. (b) Wong, M. S.; Meier, U.; Pan, F.; Gramlich, V.; Bosshard, C.; Günter, P. *Adv. Mater.* **1996**, *8*, 416–420. (c) Boldt, P.; Bourhill, G.; Bräuchle, C.; Jim, Y.; Kammler, R.; Müller, C.; Rase, J.; Wichern, J. *J. Chem. Soc., Chem. Comm.* **1996**, 793–795.

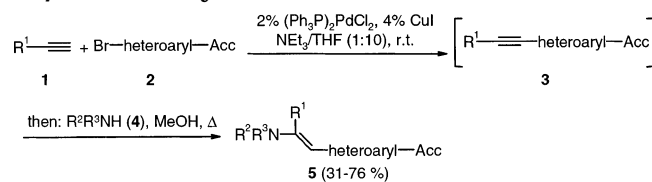
(3) (a) Effenberger, F.; Würthner, F. *Angew. Chem., Int. Ed. Engl.* **1993**, *32*, 719–721. (b) Würthner, F.; Effenberger, F.; Wortmann, R.; Krämer, P. *Chem. Phys.* **1993**, *173*, 305–314. (c) Bedworth, P. V.; Cai, Y.; Jen, A.; Marder, S. R. *J. Org. Chem.* **1996**, *61*, 2242–2246.

SCHEME 3. Comparison of Several Electron-Deficient Heteroaryl Halides in a Coupling–Aminovinylation Sequence


^a Product was identified by GC/MS analysis (100% conversion of the halide) and but not isolated.

range of functional groups.⁶ Taking advantage of this general alkyne synthesis, a retrosynthetic analysis of push–pull chromophores leads to a cross-coupling of a terminal alkyne with an electron-deficient aromatic or heteroaromatic π -electron system, furnishing a now activated electron-deficient alkyne that could undergo a Michael addition with a suitable secondary amine, preferentially in a one-pot reaction (Scheme 2).

A survey of the literature reveals that, although the Michael addition to acceptor-substituted acetylenes⁷ is a well-established methodology, especially in heterocyclic chemistry, this straightforward concept of an in-situ alkyne activation has not been explored. However, quite a number of electron-deficient arenes and heteroarenes, such as pyridines, can be coupled with alkynes in the presence of secondary amines without Michael-type product formation.^{6b} Presumably, the polarizability of the π -electron system plays a key role for opening the additional Michael-type reactivity. Therefore, phenylacetylene (**1**) and several electron-deficient heteroaryl halides **2** were subjected to typical Sonogashira coupling conditions. Upon complete conversion to the corresponding coupling products **3**, subsequent addition of pyrrolidine (**4a**) allowed for an evaluation of the electrophilic reactivity in Michael-type aminations (Scheme 3). Interestingly, among several electron-deficient heterocycles, only the nitrothienyl-substituted alkyne **3a** was successfully transformed into the amino vinylated Michael adduct **5a**. Neither the furyl aldehyde-substituted system **3d** nor pyridyl-substituted alkyne **3e** reacted in the sense of a Michael addition, not even after prolonged heating. Obviously, the choice of the electron-deficient halide is crucial for the feasibility of a consecutive Michael addition.

SCHEME 4 Coupling–Aminovinylation Sequence to β -Amino Vinyl Heteroarenes^a


As a consequence, the reaction of several (hetero)-aromatic and aliphatic terminal alkynes **1** with 2-bromo 5-nitrothiophene (**2a**), 2-bromo 5-nitrothiazole (**2h**), and 2-bromo 5-nitropyridine (**2i**) under the conditions of the Sonogashira coupling followed by subsequent addition of various secondary amines **4** furnished the acceptor-substituted enamines **5** in good yields as orange to red crystals (**5d** as a deep red oil) with an intense metallic merocyanine luster (Scheme 4, Table 1).⁸ The one-pot sequence to the push–pull chromophores proceeds smoothly even with a bisacetylene **1d** (entry 9) and also in an intramolecular fashion with a 5-amino alkyne **1e** (entry 10).

Characteristically and as an indication for the successful aminovinylation, the singlets appearing between δ 5.36 and 5.96 in the proton NMR spectra of the enamines **5** can be assigned to the enamine β -protons. Expectedly, the magnetic anisotropy of the proximal (hetero)aryl substituents and steric biases around these protons by the alkylamino fragments affect the shift of the signals. According to the ¹³C NMR spectra, the sp^2 -hybridized enamine β -methine carbon atoms can be easily identified at low field between δ 87.0 and 104.1 by intense cross-peaks in the HETCOR two-dimensional NMR experiments. In all cases the (*E*)-configured enamines **5** are formed with good to excellent stereoselectivity (dr = 4:1 to >99: <1). The (*E*)-configuration of the enamines was deduced from the appearance of strong cross-peaks in the two-dimensional NOESY experiments between the enamine β -protons and the α -protons of the amine substituents. Additionally, the (*E*)-configurations of the enamines **5** were unambiguously supported by an X-ray structure

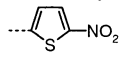
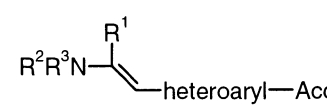
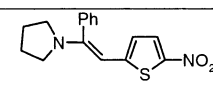
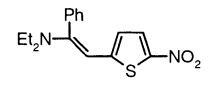
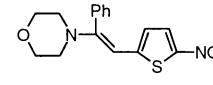
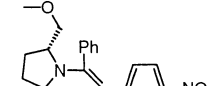
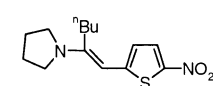
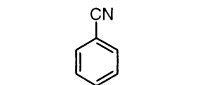
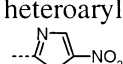
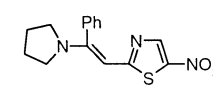
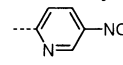
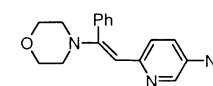
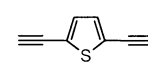
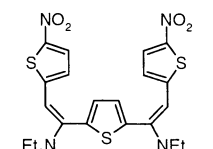
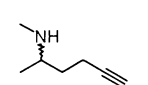
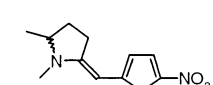
(5) (a) Müller, T. J. J.; Ansorge, M.; Aktah, D. *Angew. Chem., Int. Ed.* **2000**, *39*, 1253–1256. (b) Netz, A.; Polborn, K.; Müller, T. J. J. *Organometallics* **2001**, *20*, 376–378. (c) Müller, T. J. J. *Eur. J. Org. Chem.* **2001**, 2021–2033. (d) Braun, R. U.; Zeitler, K.; Müller, T. J. J. *Org. Lett.* **2001**, *3*, 3297–3300.

(6) (a) Takahashi, S.; Kuroyama, Y.; Sonogashira, K.; Hagihara, N. *Synthesis* **1980**, 627–629. (b) Sonogashira, K. In *Metal Catalyzed Cross-Coupling Reactions*; Diederich, F., Stang, P. J., Eds; Wiley-VCH: Weinheim, 1998; pp 203–229.

(7) Dickstein, J. I.; Miller, S. I. In *The Chemistry of the Functional Group—The Chemistry of the Carbon–Carbon Triple Bond*; Patai, S., Ed.; Wiley: Chichester, UK, 1978; Vol. 2, pp 813–955.

(8) Reaction of **5a** with (trimethyl)silyl acetylene or 2-methyl 2-propynol did not give rise to the Michael adduct.

TABLE 1. Three-Component Coupling–Aminovinylation Sequence of Alkynes 1, Heteroaryl Halides 2, and Secondary Amines 4 to Enamines 5

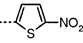
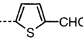
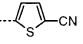
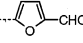
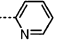
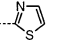
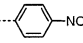
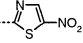
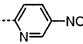
Entry	alkyne 1 $R^1-C\equiv C$	heteroaryl halide 2 Br–heteroaryl–Acc 	sec. amine 4 R^2R^3NH	enamine 5 (Yield %) 
1	$R^1 = \text{Ph}$ (1a)	heteroaryl–Acc (2a)	= pyrrolidine (4a)	 5a (57 %)
2	1a	2a	$R^2 = R^3 = \text{Et}$ (4b)	 5b (67 %)
3	1a	2a	morpholine (4c)	 5c (76 %)
4	1a	2a	(2 <i>R</i>)-methoxymethyl pyrrolidine (4d)	 5d (52 %)
5	$R^1 = \text{}^t\text{Bu}$ (1b)	2a	4a	 5e (71 %)
6	$R^1 = p\text{-C}_6\text{H}_4\text{CN}$ (1c)	2a	4c	 5f (69 %)
7	1a	heteroaryl–Acc  (2h)	= 4a	 5g (42 %)
8	1a	heteroaryl–Acc  (2i)	= 4c	 5h (69 %)
9	 1d	2a	4b	 5i (67 %)
10	 1e	2a	-	 5j (31 %)

analysis of compound **5e**.⁹ A very favorable aspect for NLO applications can be deduced from intermediate bond length alternations.¹⁰ Thus, the C–N bond lengths (1.35 and 1.39 Å) are fairly short and display a high C–N double-bond character, whereas, the C–C bond lengths (1.37–1.41 Å) lie within the margin of highly delocalized

aromatic π -electron systems (ethylene C=C, 1.32 Å; butadiene C–C, 1.48 Å).¹¹

Most peculiar for the successful coupling–aminovinylation sequence is the significant dependence on the electron-withdrawing substituent attached to the alkyne, in particular because all acetylenic ketones¹² and esters¹³

TABLE 2. Calculated (PM3) Atomic Charges from the Electrostatic Potential (ESP) and the Mulliken Natural Population Analysis (NPA), Selected Experimental ¹³C NMR Shifts (Recorded in CDCl₃, 20 °C), and Calculated (PM3) Dipole Moments and LUMO Energies.

Ph— \equiv —(hetero)aryl—Acc	β	α	C_β			C_α			$ C_\beta - C_\alpha $	Dipole moment μ [D]	LUMO [eV]	Reaction with sec. amines
			ESP	NPA	¹³ C NMR	ESP	NPA	¹³ C NMR				
heteroaryl-Acc			ESP	NPA	¹³ C NMR	ESP	NPA	¹³ C NMR	ESP	NPA	¹³ C NMR	
 3a	0.079	-0.030	98.2	-0.263	-0.141	81.1	0.342	0.111	17.1	6.777	-1.876	+
 3b	-0.030	-0.064	97.9	-0.134	-0.104	82.0	0.104	0.040	15.9	3.213	-1.331	-
 3c	0.012	-0.056	96.8	-0.203	-0.120	80.5	0.215	0.064	16.3	4.509	-1.454	-
 3d	0.029	-0.049	96.4	-0.213	-0.124	78.5	0.242	0.075	17.9	3.462	-0.958	-
 3e	0.176	-0.081	89.1	-0.503	-0.117	88.4	0.679	0.036	0.7	1.680	-0.698	-
 3f	0.244	-0.045	93.8	-0.490	-0.118	82.1	0.734	0.073	11.7	1.090	-1.100	-
 3g	-0.003	-0.057	94.5	-0.169	-0.153	87.3	0.096	0.083	7.2	6.347	-1.470	-
 3h	0.247	0.011	98.9	-0.497	-0.163	81.9	0.744	0.174	17.0	6.379	-2.159	+
 3i	0.288	-0.027	94.9	-0.610	-0.160	87.6	0.898	0.133	7.3	5.995	-1.734	+

are highly reactive toward Michael additions under mild conditions. A key issue is the high polarizability of the π -electron system that conjugates the acetylene fragment with the acceptor moiety. Although *p*-nitrophenyl acetylene reacts with secondary amines in highly dipolar aprotic solvents and at elevated temperatures,¹⁴ under the applied conditions, *p*-nitrotolane (**3g**) does not react with pyrrolidine. This observation prompted us to approach the nature of the electron-deficient alkynes **3** by taking a closer look at the ground-state electron distribution.

Therefore, we performed semiempirical calculations¹⁵ on phenylethynyl-substituted structures **3**, and the analysis was focused on the calculated atomic charges (PM3) as reflected by the electrostatic potentials (ESP), the Mulliken natural population analyses (NPA),¹⁶ the dipole moments, and LUMO energies (Table 2). Interestingly, neither are the dipole moments dominated by the polarity

of the corresponding functional group nor does the electrostatic potential at the alkyne carbon centers consistently correlate with the observed reactivity. For example, according to the electrostatic potential at the carbon center C_β , the pyridyl derivative **3e** (ESP, $C_\beta = 0.176$) and the thiazole compound **3f** (ESP, $C_\beta = 0.244$) should readily react with secondary amines. However, the relative LUMO energies and Mulliken natural population analysis considering the charge distribution with respect of the occupation of molecular orbitals¹⁷ reveal a satisfactory qualitative picture and rationalize the observed reactivity. The lower the LUMO and the more positive, i.e., less negative, the charge distribution at the carbon center C_β (NPA), the more likely the aminovinylation will proceed. The relative LUMO energy, the charge density at the site of nucleophilic attack, and the polarity of the triple bond reflected by the difference $|C_\beta - C_\alpha|$ (ESP and NPA) describe the polarizability of the electron-deficient alkyne. The ¹³C NMR shifts of the C_α and C_β carbon centers as an experimental magnitude for the charge density¹⁸ and as a measure for the propensity of **3** to participate in aminovinylations can here only be interpreted with caution. In the consanguine thiophene (**3a** ($C_\beta = 98.2$; $|C_\beta - C_\alpha| = 17.1$), **3b** ($C_\beta = 96.8$; $|C_\beta - C_\alpha| = 16.3$), **3c** ($C_\beta = 97.9$; $|C_\beta - C_\alpha| = 15.9$)) and thiazole series (**3f** ($C_\beta = 93.8$; $|C_\beta - C_\alpha| = 11.8$), **3h** ($C_\beta = 98.9$; $|C_\beta - C_\alpha| = 17.0$)), the characteristic alkyne carbon resonances and their differences allow for an estimated prediction of aminovinylation reactivity.

(9) Crystallographic data (excluding structure factors) for the structure reported in this paper have been deposited with the Cambridge Crystallographic Data Centre as supplementary publication no. CCDC-198897 (**5e**). These data can be obtained free of charge via the Internet at <http://www.ccdc.cam.ac.uk/conts/retrieving.html> (or from the CCDC, 12 Union Road, Cambridge CB2 1EZ, UK (fax, +44-1223/336-033; e-mail, deposit@ccdc.cam.ac.uk).

(10) Blanchard-Desce, M.; Alain, V.; Bedworth, P. V.; Marder, S. R.; Fort, A.; Runser, C.; Barzoukas, M.; Lebus, S.; Wortmann, R. *Chem. Eur. J.* **1997**, *3*, 1091–1104.

(11) Smith, M. B. *March's Advanced Organic Chemistry: Reactions, Mechanisms, and Structure*, 5th ed.; Wiley Interscience: New York, 2001; p 20.

(12) (a) Winterfeldt, E.; Preuss, H. *Chem. Ber.* **1966**, *99*, 450–458. (b) Vereshchagin, L. I.; Proidakov, A. G.; Gavrilov, L. D.; Kalabon, G. A. *J. Org. Chem. USSR* **1979**, *15*, 622–626.

(13) (a) Huisgen, R.; Herbig, K.; Siegl, A.; Huber, H. *Chem. Ber.* **1966**, *99*, 2526–2545. (b) Sharaf, S. M.; El-Sadany, S. K.; Hamed, E. A.; Youssef, A.-H. A. *Can. J. Chem.* **1991**, *69*, 1445–1449.

(14) Papanastassiou, Z. B.; Bruni, R. J.; White, E. *J. Med. Chem.* **1967**, *10*, 701–706.

(15) *PC Spartan Pro*; Wavefunction, Inc.: Irvine, CA, 1999.

(16) (a) Mulliken, R. S. *J. Chem. Phys.* **1955**, *23*, 1833–1840. Mulliken, R. S. *J. Chem. Phys.* **1955**, *23*, 1841–1846. Mulliken, R. S. *J. Chem. Phys.* **1955**, *23*, 2338–2342. Mulliken, R. S. *J. Chem. Phys.* **1955**, *23*, 2343–2346.

(17) Atkins, P. W. *Quantum*; VCH: Weinheim, 1993; p 193.

(18) Kalinowski, H.-O.; Berger, S.; Braun, S. *¹³C NMR Spektroskopie*; Georg Thieme Verlag: Stuttgart, 1984; Chapter 3.

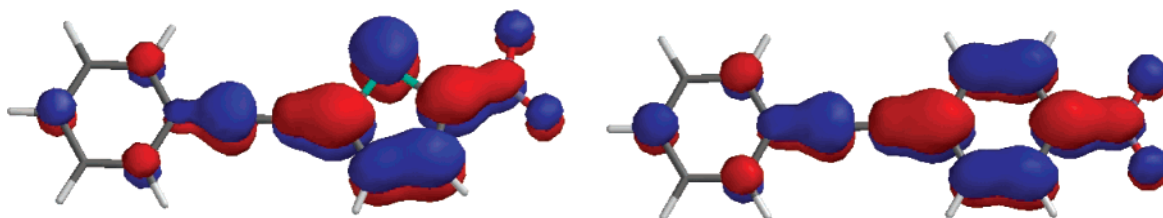


FIGURE 1. LUMOs of **3a** (−1.876 eV) and **3g** (−1.470 eV).

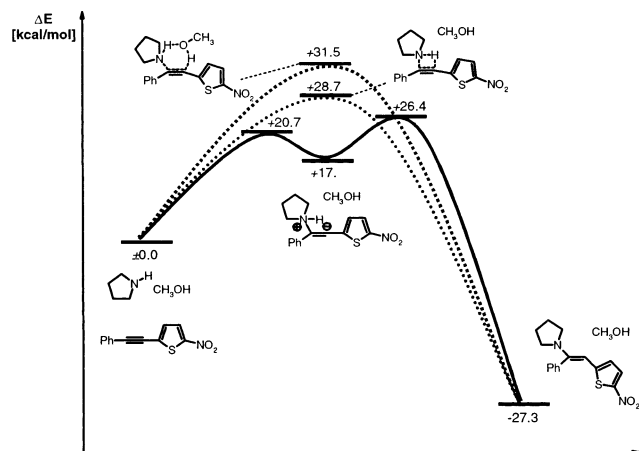


FIGURE 2. Stepwise (bold line) and concerted (trimolecular, dashed line; bimolecular, dotted line) aminovinylation of **3a** in the presence of methanol according to PM3 calculations.

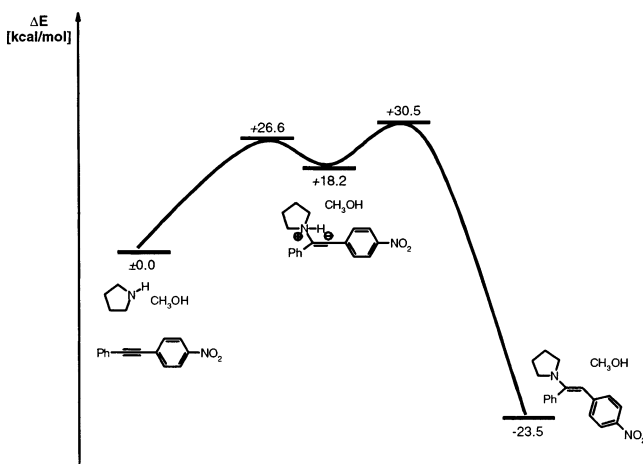


FIGURE 3. Stepwise aminovinylation of **3g** in the presence of methanol according to PM3 calculations.

According to the calculations, the rationale for the successful aminovinylation finds its borderline between the alkynes **3a** (NPA, $C_\beta = -0.030$, $|C_\beta - C_\alpha| = 0.111$; ESP, $|C_\beta - C_\alpha| = 0.342$, LUMO = −1.876 eV) and **3g** (NPA, $C_\beta = -0.057$, $|C_\beta - C_\alpha| = 0.083$; ESP, $|C_\beta - C_\alpha| = 0.096$, LUMO = −1.470 eV). In all alkynes **3**, the LUMOs show significant orbital coefficients at C_β , the preferred site of a nucleophilic attack (Figure 1).

Therefore, the pyrrolidine additions of the two borderline cases (**3a**, Figure 2; **3g**, Figure 3) were modeled by calculations on a semiempirical level of theory¹⁵ (PM3) in order to reveal the energetic aspects that could help to rationalize the observed differences in reactivity. Inspired by additions of amines to ynones in polar protic solvents¹⁴ where a six-membered transition state was

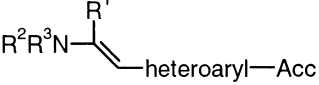
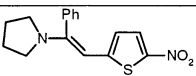
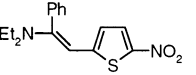
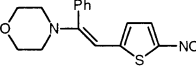
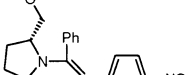
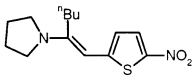
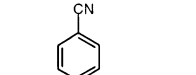
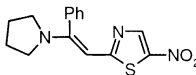
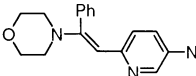
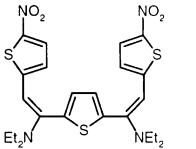
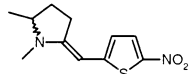
suggested for concerted aminovinylation,^{13b} we calculated several reaction pathways (relative energies of educts, transition states, and intermediates) for the trimolecular reaction of pyrrolidine, alkyne **3a**, and methanol (assuming that methanol could participate in the reaction or stabilize dipolar intermediates). Interestingly, the concerted reaction pathways proceeding through six-membered ($\Delta E_a^\ddagger = +31.5$ kcal/mol) or four-membered ($\Delta E_a^\ddagger = +28.7$ kcal/mol) transition states are higher in energy than the transition states ($\Delta E_{a,1}^\ddagger = +20.7$ kcal/mol, $\Delta E_{a,2}^\ddagger = +26.4$ kcal/mol) and the zwitterionic intermediate ($\Delta E = +17.3$ kcal/mol) of a stepwise mechanism. Furthermore, the rate-determining step of this aminovinylation is not the addition of the amine to the alkyne but the proton migration from the ammonium nitrogen atom to the highly stabilized vinyl anion. Both transition states structurally resemble the dipolar intermediate, and thus the polarity of the reaction medium should experimentally (as shown in Schemes 3 and 4) cause a further lowering of both the transition states and the intermediate.

Transposing these findings to the calculation of the trimolecular reaction of pyrrolidine, alkyne **3g**, and methanol makes it apparent that the reduced polarizability of phenylene bridge^{1a} in **3g** increases not only the energy of the dipolar intermediate (**3g**, $\Delta E = +18.2$ kcal/mol; **3a**, $\Delta E = +17.3$ kcal/mol) but also the corresponding transition state energies ($\Delta E_{a,1}^\ddagger = +26.6$ kcal/mol, $\Delta E_{a,2}^\ddagger = +30.5$ kcal/mol). Thus, both the ground-state and transition-state properties of the alkyne intermediates **3** formed by the cross-coupling step in the coupling–aminovinylation sequence allow a qualitative rationalization of the dependence of the concluding amine addition on the electronic nature of the (hetero)aryl substituents.

The synthetic application of this novel one-pot coupling–aminovinylation sequence now opens straightforward access to push–pull chromophores **5** with a flexible substitution pattern (Table 3). Expectedly, the acceptor-substituted enamines **5** display not only remarkable solvochromicities ($\Delta\tilde{\nu}(\text{acetonitrile-diethyl ether}) = 1300\text{--}2200\text{ cm}^{-1}$) but also a wide range in the long-wavelength absorption maxima ($\Delta\lambda_{\text{max}} = 404\text{--}499\text{ nm}$ (diethyl ether)). The consanguine series of pyrrolidinyl enamines **5a**, **5d**, **5e**, and **5g** reveal a linear correlation between the calculated (ZINDO/CI calculations on AM1-optimized structures **5**)¹⁹ and experimental long-wavelength absorption maxima (Figure 4) in both a polar (acetonitrile) and a less polar solvent (diethyl ether). Additionally, this semiquantitative correlation allows for optimization and fine-tuning of tailor-made NLO chromophores for mul-

(19) Calculated with AM1-optimized structures (ref 12) using Quantum CHChe Program 3.0 (Oxford Molecular Group: Oxford, 1997).

TABLE 3. Experimental (Recorded in Diethyl Ether and Acetonitrile at 20 °C) and Calculated (ZINDO/CI Calculations on AM1-Optimized Structures) UV/vis Spectroscopic Data and Solvochromicity of Push–Pull Chromophores 5

	λ_{\max} [nm] (ϵ) in Et ₂ O	λ_{\max} [nm] (ϵ) in CH ₃ CN	λ_{\max} [nm] calc.	$\Delta\tilde{\nu}$ [cm ⁻¹]
Push-pull chromophores 5				
	5a 491 (32200)	537 (37100)	431	+1800
	5b 485 (27000)	553 (37100)	-	+2500
	5c 450 (20900)	498 (21700)	-	+2100
	5d 485 (21000)	528 (24300)	429	+1700
	5e 499 (20400)	545 (43700)	434	+1700
	5f 439 (18100)	486 (21000)	-	+2200
	5g 468 (14200)	500 (17500)	419	+1400
	5h 404 (23400)	426 (20400)	-	+1300
	5i 485 (21000)	518 (44100)	-	+1300
	5j 487 (29200)	532 (34300)	-	+1700

tiple photonic applications using rapid semiempirical quantum mechanical calculations. The challenge, however, remains the availability of tailor-made materials, an issue that can be addressed by implementing one-pot multicomponent reactions that can enhance the structural diversity necessary for fine-tuning additional parameters highly desired in photorefractive materials for holographic²⁰ recording such as solubility, glass-forming properties, long-term stability, and processibility.

In conclusion, we have developed a straightforward, one-pot coupling–aminovinylation sequence to highly solvochromic enamine push–pull chromophores. According to semiempirical calculations, the aminovinylation

proceeds in a stepwise fashion through an initial zwitterionic intermediate, followed by a subsequent rate-determining intramolecular protonation. The relative LUMO energy and the ground-state charge distribution at the β -alkynyl carbon center significantly affects the success of the amine addition step as exemplified by comparative Mulliken population analyses of the charge density of investigated systems. Besides application of this novel multicomponent approach to a combinatorial

(20) Meerholz, K.; Kippelen, B.; Peyghambarian, N. In *Electrical and Optical Polymer Systems*; Wise, D. L., Wnek, G. E., Trantolo, D. J., Gresser, J. D., Cooper, T. M., Eds.; World Scientific: River Edge, NJ, 1998, pp 571–631.

TABLE 4. Experimental Details of the One-Pot Coupling–Aminovinylolation Reaction to Enamines **5** or Alkynes **3**, Respectively

entry	alkyne 1	heteroaryl halide 2	secondary amine 4	alkyne 3 /enamine 5 (yield %)
1	0.12 mL (1.10 mmol) of 1a	208 mg (1.00 mmol) of 2a	0.17 mL (2.00 mmol) of 4a	170 mg (57%) of 5a
2	0.12 mL (1.10 mmol) of 1a	190 mg (1.00 mmol) of 2b	0.17 mL (2.00 mmol) of 4a	3b ^a
3	0.12 mL (1.10 mmol) of 1a	188 mg (1.00 mmol) of 2c	0.17 mL (2.00 mmol) of 4a	3c ^a
4	0.12 mL (1.10 mmol) of 1a	159 mg (1.00 mmol) of 2d	0.17 mL (2.00 mmol) of 4a	171 mg (87%) of 3d
5	0.12 mL (1.10 mmol) of 1a	158 mg (1.00 mmol) of 2e	0.17 mL (2.00 mmol) of 4a	3e ^a
6	0.12 mL (1.10 mmol) of 1a	0.09 mL (1.00 mmol) of 2f	0.17 mL (2.00 mmol) of 4a	3f ^a
7	0.12 mL (1.10 mmol) of 1a	158 mg (1.00 mmol) of 2g	0.17 mL (2.00 mmol) of 4a	3g ^a
7	0.12 mL (1.10 mmol) of 1a	208 mg (1.00 mmol) of 2a	0.21 mL (2.00 mmol) of 4b	202 mg (67%) of 5b
8	0.12 mL (1.10 mmol) of 1a	208 mg (1.00 mmol) of 2a	0.17 mL (2.00 mmol) of 4c	240 mg (76%) of 5c
9	0.12 mL (1.10 mmol) of 1a	208 mg (1.00 mmol) of 2a	0.25 mL (2.00 mmol) of 4d	175 mg (52%) of 5d
10	0.13 mL (1.10 mmol) of 1b	208 mg (1.00 mmol) of 2a	0.17 mL (2.00 mmol) of 4a	200 mg (71%) of 5e
11	140 mg (1.10 mmol) of 1c	208 mg (1.00 mmol) of 2a	0.17 mL (2.00 mmol) of 4c	235 mg (69%) of 5f
12	0.12 mL (1.10 mmol) of 1a	209 mg (1.00 mmol) of 2h	0.17 mL (2.00 mmol) of 4a	125 mg (42%) of 5g
13	0.12 mL (1.10 mmol) of 1a	203 mg (1.00 mmol) of 2i	0.17 mL (2.00 mmol) of 4c	202 mg (69%) of 5h
14	132 mg (1.00 mmol) of 1d	416 mg (2.00 mmol) of 2a	0.42 mL (4.00 mmol) of 4b	356 mg (67%) of 5i
15	122 mg (1.10 mmol) of 1e	208 mg (1.00 mmol) of 2a		74 mg (31%) of 5j

^a Alkyne **3** was identified by GC/MS analysis (100% conversion of the halide) but not isolated.

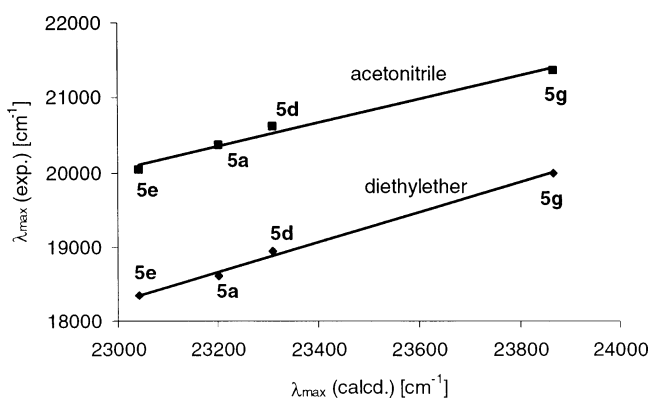


FIGURE 4. Linear correlation between calculated (abscissa; ZINDO/CI calculations on AM1-optimized structures **5**) and experimental (ordinate, recorded in diethyl ether (clubs), $R^2 = 0.9856$, and acetonitrile (squares), $R^2 = 0.9968$) long-wavelength absorption maxima λ_{\max} .

development of novel NLO chromophores for use in photorefractive devices, the potential applications of in-situ alkyne activation for the design of novel multicomponent reactions to improve and simplify organic synthetic methodology are numerous. Studies addressing these issues are currently under investigation.

Experimental Section

All reactions involving water-sensitive compounds were carried out in oven-dried Schlenk glassware under a nitrogen atmosphere. The solvents were dried according to standard procedures²¹ and distilled prior to use. Column chromatography: aluminum oxide 5016 A basic. Thin-layer chromatography (TLC): aluminum oxide-layered aluminum foil. Melting points are uncorrected. Phenylacetylene (**1a**), 1-hexyne (**1b**), trimethylsilylacetylene, 2-bromopyridine (**2e**), 2-bromo-5-nitrothiazole (**2h**), 2-bromo-5-nitropyridine (**2i**), and the applied secondary amines were purchased and used without further purification. 2-Bromo-5-nitrothiophene (**2a**),²² 2-bromo-5-cyanothiophene (**2c**),²³ 2-bromo-5-furfural (**2d**),²⁴ and 2,5-diethylthiophene (**1d**)²⁵ were synthesized according to literature

(21) *Organikum*, 20th ed.; Becker, H. G. O.; Berger, W.; Domschke, G.; Fanghänel, E.; Faust, J.; Fischer, M.; Gentz, F.; Gewalt, K.; Gluch, R.; Mayer, R.; Müller, K.; Pavel, D.; Schmidt, H.; Schollberg, K.; Schwetlick, K.; Seiler, E.; Zeppenfeld, G.; Johann Ambrosius Barth Verlag: Heidelberg, Leipzig, 1996.

procedures. *p*-Cyanophenylacetylene (**1c**) and the acceptor-substituted heteroaryl phenylacetylenes **3** were prepared by Sonogashira coupling of the corresponding bromo or iodo derivatives and TMS acetylene or phenylacetylene and subsequent alkaline desilylation (**1c**) in excellent yield.⁶ *N*-Methyl-1-methyl-4-pentynylamine (**1e**) was prepared in analogy to published procedures.²⁶ ¹H and ¹³C NMR spectra were obtained with DMSO-*d*₆ and CDCl₃ as solvents. The assignments of quaternary C, CH, CH₂, and CH₃ were made on the basis of DEPT spectra. Elemental analyses were carried out in the microanalytical laboratory of the Department Chemie der Ludwig-Maximilians-Universität München.

General Procedure for the Sonogashira Coupling–Aminovinylolation Sequence. To a stirred mixture of the heteroaryl bromide **2** (1 mmol), 14 mg (0.02 mmol) of Pd(PPh₃)₂Cl₂, and 7 mg (0.04 mmol) of CuI in a mixture of 5 mL of THF and 1 mL of triethylamine under nitrogen was added dropwise over 10 min a solution of the acetylene **1** (1.1 mmol) in 5 mL of THF. The reaction mixture was stirred at room temperature for 6 h until the complete consumption of **2** (monitored by TLC or GC-MS). Then, a solution of the amine **4** (2 mmol) in 5 mL of methanol was added, and the reaction mixture was heated to reflux temperatures for 3–6 h until the complete conversion of the intermediate alkyne **3** (monitored by TLC or GC-MS). The solvents were evaporated in vacuo, and the residue was chromatographed over a short pad of aluminum oxide eluting with dichloromethane to furnish after recrystallization from hexane/chloroform the analytically pure enamines **5** as crystalline solids (see Table 4 for experimental details).

(E)-1-[2-(5-Nitrothien-2-yl)-1-phenyl-vinyl]pyrrolidine (5a**).** *E/Z* = 60:1 (¹H NMR, minor diastereomer not entered). Crystals with a green metallic luster, mp 169–170 °C. ¹H NMR (CDCl₃, 400 MHz): δ 1.90–1.98 (m, 4 H), 3.18–3.26 (m, 4 H), 5.51 (s, 1 H), 6.20 (d, *J* = 4.6 Hz, 1 H), 7.25–7.29 (m, 2 H), 7.51–7.57 (m, 4 H). ¹³C NMR (CDCl₃, 100 MHz): δ 25.3 (CH₂), 49.0 (CH₂), 92.8 (CH), 120.5 (CH), 126.5 (C_{quat}), 128.4 (CH), 130.2 (CH), 130.3 (CH), 130.3 (CH), 135.5 (C_{quat}), 153.7 (C_{quat}), 157.0 (C_{quat}). EI MS (70 eV, *m/z* (%)): 300 (M⁺, 100), 254 (M⁺ – NO₂, 21), 184 (M⁺ – NO₂ – N(C₂H₄)₂, 22). IR (KBr): $\tilde{\nu}$ 1557, 1437, 1273, 1166, 1114, 1040 cm⁻¹. UV/

(22) Seed, A. J.; Toyne, K. J.; Goodby, J. W.; Hird, M. *J. Mater. Chem.* **2000**, *10*, 2069–2080.

(23) Seed, A. J.; Toyne, K. J.; Goodby, J. W. *J. Mater. Chem.* **1995**, *5*, 653–661.

(24) Märkl, G.; Knott, T.; Kreitmeier, P.; Burgemeister, T.; Kastner, F. *Tetrahedron* **1996**, *52*, 11763–11782.

(25) Lewis, J.; Long, N. J.; Raithby, P. R.; Shields, G. P.; Wong, W.; Younus, M. *J. Chem. Soc., Dalton Trans* **1997**, 4283–4288.

(26) Tokuda, M.; Fujita, H.; Nitta, M.; Suiginome, H. *Heterocycles* **1996**, *42*, 385–395.

vis (CH₃CN): λ_{\max} (ϵ) 537 nm (37 100). UV/vis (ether): λ_{\max} (ϵ) 491 nm (32200). Anal. Calcd for C₁₆H₁₆N₂O₂S (300.38): C, 63.98; H, 5.37; N, 9.33; S, 10.67. Found: C, 63.92; H, 5.31; N, 9.19; S, 10.95.

(E)-Diethyl-[2-(5-nitrothien-2-yl)-1-phenyl-vinyl]-amine (5b). *E/Z* = 9:1 (¹H NMR, minor diastereomer not entered). Red brown crystals with a metallic luster, mp 157–158 °C. ¹H NMR (CDCl₃, 400 MHz): δ 1.15 (t, *J* = 7.1 Hz, 6 H), 3.21 (q, *J* = 7.1 Hz, 4 H), 5.63 (s, 1 H), 6.21 (d, *J* = 4.6 Hz, 1 H), 7.22–7.26 (m, 2 H), 7.52–7.58 (m, 4 H). ¹³C NMR (CDCl₃, 100 MHz): δ 13.2 (CH₃), 44.1 (CH₂), 93.1 (CH), 120.7 (CH), 129.00 (CH), 129.1 (C_{quat}), 129.9 (CH), 130.3 (CH), 130.3 (CH), 134.6 (C_{quat}), 154.4 (C_{quat}), 156.9 (C_{quat}). EI MS (70 eV, *m/z* (%)): 302 (M⁺, 100), 273 (M⁺ – C₂H₅, 12), 256 (M⁺ – NO₂, 66), 184 (M⁺ – NO₂, – N(C₂H₅)₂, 27). IR (KBr): $\tilde{\nu}$ 1553, 1430, 1288, 1267, 1243, 1122, 1096, 1042 cm⁻¹. UV/vis (CH₃CN): λ_{\max} (ϵ) 533 nm (37100). UV/vis (ether): λ_{\max} (ϵ) 485 nm (27000). Anal. Calcd for C₁₆H₁₈N₂O₂S (302.40): C, 63.55; H, 6.00; N, 9.26; S, 10.60. Found: C, 63.20; H, 5.91; N, 9.16; S, 10.64.

(E)-4-[2-(5-Nitrothien-2-yl)-1-phenyl-vinyl]morpholine (5c). *E/Z* = 20:1 (¹H NMR, minor diastereomer not entered). Crystals with a green metallic luster, mp 147–148 °C. ¹H NMR (CDCl₃, 400 MHz): δ 3.07 (t, *J* = 4.9 Hz, 4 H), 3.71 (t, *J* = 4.9 Hz, 4 H), 5.73 (s, 1 H), 6.33 (d, *J* = 4.6 Hz, 1 H), 7.25–7.30 (m, 2 H), 7.48–7.56 (m, 4 H). ¹³C NMR (CDCl₃, 100 MHz): δ 48.1 (CH₂), 66.5 (CH₂), 96.6 (CH), 122.6 (CH), 128.4 (C_{quat}), 129.3 (CH), 129.6 (CH), 130.1 (CH), 130.5 (CH), 134.3 (C_{quat}), 153.8 (C_{quat}), 155.1 (C_{quat}). EI MS (70 eV, *m/z* (%)): 316 (M⁺, 100), 270 (M⁺ – NO₂, 28), 184 (M⁺ – NO₂, – C₄H₈NO, 44). IR (KBr): $\tilde{\nu}$ 1570, 1431, 1298, 1232, 1137, 1111, 1040, 1018 cm⁻¹. UV/vis (CH₃CN): λ_{\max} (ϵ) 498 nm (21700). UV/vis (ether): λ_{\max} (ϵ) 450 nm (20900). Anal. Calcd for C₁₆H₁₆N₂O₃S (316.38): C, 60.74; H, 5.10; N, 8.85; S, 10.13. Found: C, 60.38; H, 5.07; N, 8.67; S, 10.54.

(E)-1-[2-(5-Nitrothien-2-yl)-1-phenyl-vinyl]-2(R)-methoxymethyl Pyrrolidine (5d). Only the (*E*)-stereoisomer (¹H NMR). Deep red oil. ¹H NMR (CDCl₃, 400 MHz): δ 1.84–1.98 (m, 4 H), 3.07–3.26 (m, 7 H), 3.70–3.76 (m, 1 H), 5.53 (s, 1 H), 6.16 (d, *J* = 4.6 Hz, 1 H), 7.14–7.26 (m, 2 H), 7.45–7.50 (m, 4 H). ¹³C NMR (CDCl₃, 100 MHz): δ 22.0 (CH₂), 27.4 (CH₂), 48.5 (CH₂), 57.3 (CH), 58.0 (CH₃), 72.1 (CH₂), 93.0 (CH), 119.9 (CH), 127.4 (CH), 128.3 (CH), 129.0 (CH), 129.2 (CH), 131.1 (C_{quat}), 133.9 (C_{quat}), 152.1 (C_{quat}), 155.4 (C_{quat}). EI MS (70 eV, *m/z* (%)): 344 (M⁺, 19), 299 (M⁺ – CH₂OCH₃, 86), 267 (M⁺ – OCH₃, – NO₂, 100). IR (KBr): $\tilde{\nu}$ 1559, 1435, 1276, 1170, 1120, 1036 cm⁻¹. UV/vis (CH₃CN): λ_{\max} (ϵ) 528 nm (24300). UV/vis (ether): λ_{\max} (ϵ) 485 nm (21000). HRMS calcd for C₁₈H₂₀N₂O₃S, 344.1190; found 344.1205.

(E)-1-[2-(5-Nitrothien-2-yl)-1-butyl-vinyl]pyrrolidine (5e). Only the (*E*)-stereoisomer (¹H NMR). Crystals with a blue metallic luster, mp 100–101 °C. ¹H NMR (CDCl₃, 400 MHz): δ 0.99 (t, *J* = 7.0 Hz, 3 H), 1.50–1.64 (m, 4 H), 1.96–2.02 (m, 4 H), 2.62–2.67 (m, 2 H), 3.36–3.46 (m, 4 H), 5.36 (s, 1 H), 6.42 (d, *J* = 4.7 Hz, 1 H), 7.73 (d, *J* = 4.7 Hz, 1 H). ¹³C NMR (CDCl₃, 100 MHz): δ 13.8 (CH₃), 23.0 (CH₂), 25.2 (CH₂), 29.0 (CH₂), 31.2 (CH₂), 48.3 (CH₂), 92.6 (CH), 120.3 (CH), 131.1 (CH), 128.2 (C_{quat}), 155.6 (C_{quat}), 156.2 (C_{quat}). EI MS (70 eV, *m/z* (%)): 280 (M⁺, 6), 217 (M⁺ – NO₂, – CH₃, – 2H, 100). IR (KBr): $\tilde{\nu}$ 1557, 1442, 1286, 1162, 1126, 1092, 1042 cm⁻¹. UV/vis (CH₃CN): λ_{\max} (ϵ) 545 nm (43700). UV/vis (ether): λ_{\max} (ϵ) 499 nm (20400). Anal. Calcd for C₁₄H₂₀N₂O₂S (280.39): C, 59.97; H, 7.19; N, 9.99; S, 11.44. Found: C, 59.80; H, 7.08; N, 9.96; S, 11.57.

(E)-4-[2-[5-Nitrothien-2-yl]-1-(4-cyano)phenyl-vinyl]-morpholine (5f). *E/Z* = 4:1 (¹H NMR). Red crystals, mp 222–223 °C. ¹H NMR (CDCl₃, 400 MHz): δ 2.94 (t, *J* = 4.9 Hz, 4 H), 3.66 (t, *J* = 4.9 Hz, 4 H), 5.70 (s, 1 H), 6.28 (d, *J* = 4.6 Hz, 1 H), 7.41 (d, *J* = 8.4 Hz, 2 H), 7.51 (d, *J* = 4.6 Hz, 1 H), 7.73 (d, *J* = 8.4 Hz, 2 H). Additional ¹H NMR signals for the minor isomer: δ 3.18 (t, *J* = 4.8 Hz, 2 H), 3.22 (t, *J* = 4.9 Hz, 2 H), 3.74 (t, *J* = 4.8 Hz, 2 H), 3.96 (t, *J* = 4.9 Hz, 2 H), 5.21 (s, 1 H), 5.92 (d, *J* = 4.6 Hz, 1 H). ¹³C NMR (CDCl₃, 100 MHz): δ

48.4 (CH₂), 66.4 (CH₂), 98.0 (CH), 114.3 (C_{quat}), 118.0 (C_{quat}), 123.5 (CH), 129.2 (CH), 130.9 (CH), 133.6 (CH), 139.4 (C_{quat}), 151.4 (C_{quat}), 152.6 (C_{quat}). Additional ¹³C NMR signals for the minor isomer: δ 43.2 (CH₂), 49.1 (CH₂), 63.8 (CH₂), 65.7 (CH₂), 102.9 (CH), 128.8 (CH), 132.8 (CH). EI MS (70 eV, *m/z* (%)): 341 (M⁺, 100), 295 (M⁺ – NO₂, 17), 209 (M⁺ – NO₂, – C₄H₈NO, 27), 102 (4-CN – Ph, 11). IR (KBr): $\tilde{\nu}$ 1579, 1429, 1303, 1227, 1170, 1110, 1023, 892 cm⁻¹. UV/vis (CH₃CN): λ_{\max} (ϵ) 486 nm (21000). UV/vis (ether): λ_{\max} (ϵ) 439 nm (18100). Anal. Calcd for C₁₇H₁₅N₃O₃S (341.39): C, 59.81; H, 4.43; N, 12.31; S, 9.39. Found: C, 59.56; H, 4.38; N, 12.17; S, 9.43.

(E)-1-[2-(5-Nitrothiazol-2-yl)-1-phenyl-vinyl]pyrrolidine (5g). Only the (*E*)-stereoisomer (¹H NMR). Red crystals, mp 132–133 °C. ¹H NMR (CDCl₃, 400 MHz): δ 1.80–2.20 (m, 4 H), 3.10–3.60 (m, 4 H), 5.96 (s, 1 H), 7.27–7.30 (m, 2 H), 7.59–7.63 (m, 3 H), 8.19 (s, 1 H). ¹³C NMR (CDCl₃, 100 MHz): δ 25.2 (CH₂), 49.4 (CH₂), 95.0 (CH), 127.7 (CH), 130.96 (CH), 130.99 (CH), 134.3 (C_{quat}), 141.2 (C_{quat}), 143.7 (CH), 158.5 (C_{quat}), 174.7 (C_{quat}). EI MS (70 eV, *m/z* (%)): 301 (M⁺, 40), 255 (M⁺ – NO₂, 100), 232 (M⁺ – N(C₂H₄)₂, 14). IR (KBr): $\tilde{\nu}$ 1548, 1456, 1264, 1207, 1175, 1108 cm⁻¹. UV/vis (CH₃CN): λ_{\max} (ϵ) 500 nm (17500). UV/vis (ether): λ_{\max} (ϵ) 468 nm (14200). Anal. Calcd for C₁₅H₁₅N₃O₃S (341.39): C, 59.78; H, 5.02; N, 13.94; S, 10.64. Found: C, 59.89; H, 5.16; N, 13.55.

(E)-4-[2-(5-Nitropyrid-2-yl)-1-phenyl-vinyl]morpholine (5h). *E/Z* = 13:1 (¹H NMR). Orange crystals, mp 109–110 °C. ¹H NMR (CDCl₃, 400 MHz): δ 3.06 (t, *J* = 4.8 Hz, 4 H), 3.68 (t, *J* = 4.9 Hz, 4 H), 5.80 (s, 1 H), 6.10 (d, *J* = 9.2 Hz, 1 H), 7.21–7.25 (m, 2 H), 7.32–7.41 (m, 3 H), 7.73 (dd, *J* = 2.6 Hz, *J* = 9.2 Hz, 1 H), 9.06 (d, *J* = 2.6 Hz, 1 H). Additional ¹H NMR signals for the minor isomer: δ 3.14 (t, *J* = 4.9 Hz, 4 H), 3.95 (t, *J* = 4.9 Hz, 4 H), 5.41 (s, 1 H), 6.19 (d, *J* = 4.5 Hz, 1 H). ¹³C NMR (CDCl₃, 100 MHz): δ 46.7 (CH₂), 66.6 (CH₂), 104.1 (CH), 120.3 (CH), 128.6 (C_{quat}), 129.5 (CH), 129.6 (CH), 129.7 (CH), 129.9 (CH), 135.3 (C_{quat}), 145.1 (CH), 158.4 (C_{quat}), 164.5 (C_{quat}). Additional ¹³C NMR signals for the minor isomer: δ 43.3 (CH₂), 63.9 (CH₂), 94.2 (CH), 126.1 (CH), 128.6 (CH), 130.8 (CH). EI MS (70 eV, *m/z* (%)): 311 (M⁺, 55), 265 (M⁺ – NO₂, 16), 225 (M⁺ – C₄H₈NO, 100), 179 (M⁺ – NO₂, – C₄H₈NO, 62). IR (KBr): $\tilde{\nu}$ 1581, 1558, 1508, 1337, 1280, 1244, 1198, 1107, 1022 cm⁻¹. UV/vis (CH₃CN): λ_{\max} (ϵ) 426 nm (20400). UV/vis (ether): λ_{\max} (ϵ) 404 nm (23400). Anal. Calcd for C₁₇H₁₇N₃O₃ (311.34): C, 65.58; H, 5.50; N, 13.50. Found: C, 65.64; H, 5.63; N, 13.00.

(E,E)-2,5-Bis[2-(5-nitrothien-2-yl)-1-diethylamino-vinyl]-thiophene (5i). *E,E/Z* = 8:1 (¹H NMR, minor diastereomer not entered). Violet crystals, mp 206–207 °C. ¹H NMR (CDCl₃, 400 MHz): δ 1.24 (t, *J* = 7.0 Hz, 12 H), 3.47 (q, *J* = 7.0 Hz, 8 H), 5.78 (s, 2 H), 6.51 (d, *J* = 4.5 Hz, 2 H), 7.24 (s, 2 H), 7.64 (d, *J* = 4.5 Hz, 2 H). ¹³C NMR (CDCl₃, 100 MHz): δ 13.3 (CH₃), 44.6 (CH₂), 96.0 (CH), 121.9 (CH), 129.6 (CH), 131.9 (CH), 138.7 (C_{quat}), 144.0 (C_{quat}), 145.0 (C_{quat}), 154.9 (C_{quat}). EI MS (70 eV, *m/z* (%)): 532 (M⁺, 100), 486 (M⁺ – NO₂, 39). IR (KBr): $\tilde{\nu}$ 1568, 1430, 1290, 1240, 1166, 1195, 1037 cm⁻¹. UV/Vis (CH₃CN): λ_{\max} (ϵ) 518 nm (44100). UV/Vis (ether): λ_{\max} (ϵ) 485 nm (21000). Anal. Calcd for C₂₄H₂₈N₄O₄S₃ (532.71): C 54.11, H 5.30, N 10.52, S 18.06. Found: C 53.90, H 5.12, N 10.18, S 17.95.

rac-2-(5-Nitrothien-2-ylidene)-1,5-dimethylpyrrolidine (5j). Only the (*E*)-stereoisomer (¹H NMR). Violet crystals, mp 127–128 °C. ¹H NMR (CDCl₃, 400 MHz): δ 1.23 (d, *J* = 6.4 Hz, 3 H), 1.67–1.76 (m, 1 H), 2.24–2.34 (m, 1 H), 2.79–2.95 (m, 5 H), 3.64–3.72 (m, 1 H), 5.37 (s, 1 H), 6.44 (d, *J* = 4.8 Hz, 1 H), 7.76 (d, *J* = 4.8 Hz, 1 H). ¹³C NMR (CDCl₃, 100 MHz): δ 19.2 (CH₃), 29.2 (CH₂), 31.1 (CH₂), 31.3 (CH₃), 60.8 (CH), 87.0 (CH), 119.1 (CH), 131.4 (CH), 141.7 (C_{quat}), 157.6 (C_{quat}), 157.8 (C_{quat}). EI MS (70 eV, *m/z* (%)): 238 (M⁺, 100), 223 (M⁺ – CH₃, 62), 208 (M⁺ – 2CH₃, 27), 192 (M⁺ – NO₂, 21), 150 (M⁺ – 2CH₃, – NO₂, 19). IR (KBr): $\tilde{\nu}$ 1585, 1447, 1325, 1299, 1251, 1168, 1131, 1034 cm⁻¹. UV/vis (CH₃CN): λ_{\max} (ϵ) 532 nm (34300). UV/vis (ether): λ_{\max} (ϵ) 487 nm (29200). Anal.

Calcd for C₁₁H₁₄N₂O₂S (238.31): C, 55.44; H, 5.92; N, 11.76; S, 13.45. Found: C, 55.13; H, 5.84; N, 11.72; S, 13.58.

Acknowledgment. Financial support of this work by the Fonds der Chemischen Industrie is gratefully acknowledged.

Supporting Information Available: ¹H NMR spectra of compounds **5**, computational data of alkynes **3** and enamines

5, and the stationary points of several reaction pathways, an ORTEP plot, tables of data collection parameters, bond lengths and angles, positional and thermal parameters, and least-squares planes for **5e**. This material is available free of charge via the Internet at <http://pubs.acs.org>.

JO0264700